EUROPEAN ORGANIZATION FOR NUCLEAR RESEARCH

CERN-EP/82-27
3 March 1982

MEASUREMENTS OF ELASTIC SCATTERING IN ALPHA-ALPHA AND ALPHA-PROTON COLLISIONS AT THE CERN INTERSECTING STORAGE RINGS

M. Ambrosio[2)], G. Anzivino[2)], G. Barbarino[2)], U. Becker[1,*)]
G. Carboni[3)], V. Cavasinni[**)], T. Del Prete[3)], G. Kantardjian[1)],
D. Lloyd Owen[1,4)], M. Morganti[3)], J. Paradiso[1,†)], G. Paternoster[2)],
S. Patricelli[2)], M. Steuer[††)], and M. Valdata-Nappi[3)]

[CERN[1)] - Napoli[2)] - Pisa[3)] - Stony Brook[4)] Collaboration]

ABSTRACT

We measured the elastic scattering of $\alpha\alpha$ at $\sqrt{s}$ = 126 GeV and of αp at $\sqrt{s}$ = 89 GeV. For $\alpha\alpha$, the differential cross-section $d\sigma/dt$ has a diffractive pattern with minima at $|t|$ = 0.10 and 0.38 GeV^2. At small $|t|$ = 0.05–0.07 GeV^2, this cross-section behaves like $e^{(100\pm10)t}$. Extrapolating a fit to the data to the optical point, we obtained for the total cross-section $\alpha_{tot}(\alpha\alpha)$ = 250 ± 50 mb and an integrated elastic cross-section $\sigma_{el}(\alpha\alpha)$ = 45 ± 15 mb. Another method of estimating $\sigma_{tot}(\alpha\alpha)$, based on measuring the interaction rate, yielded 295 ± 40 mb. For αp, $d\sigma/dt$ has a minimum at $|t|$ = 0.20 GeV^2, and for $0.05 < |t| < 0.18$ GeV^2 behaves like $e^{(41\pm2)t}$. Extrapolating this slope to $|t| = 0$, we found $\sigma_{tot}(\alpha p)$ = 130 ± 20 and $\sigma_{el}(\alpha p)$ = 20 ± 4 mb. Results on pp elastic scattering at $\sqrt{s}$ = 63 GeV agree with previous ISR experiments.

(Submitted to Physics Letters B)

---

1) CERN, Geneva, Switzerland.

2) Istituto di Fisica dell'Università, Napoli, and INFN, Sezione di Napoli, Italy.

3) INFN, Sezione di Pisa and Istituto di Fisica dell'Università, Pisa, Italy.

4) State University of New York, Stony Brook, NY, USA.

*) Present address: Lab. for Nuclear Science, MIT, Cambridge, Mass., USA.

**) Istituto di Fisica, Università di Bologna, Italy; now at the Scuola Normale Superiore, Pisa, Italy.

†) Present address: ETH, Zürich, Switzerland.

††) LAPP, Annecy, France; now at the Institut für Hochenergiephysik der Österreichischen Akademie der Wissenschaften, Vienna, Austria.

The storage of α-particle beams in the CERN Intersecting Storage Rings (ISR) enabled us to study αα and αp interactions at unprecedentally high centre-of-mass energies. We used a small-angle detector to measure the elastic scattering of αα at $\sqrt{s}$ = 126 GeV in the four-momentum-transfer range $0.05 < |t| < 0.8$ GeV^2, and for αp at $\sqrt{s}$ = 89 GeV in the range $0.05 < |t| < 0.25$ GeV^2. The luminosities achieved were $L \sim 3 \times 10^{28}$ cm^{-2} s^{-1} for αα and $L \sim 50 \times 10^{28}$ cm^{-2} s^{-1} for αp. Companion data for pp elastic scattering were also collected at $\sqrt{s}$ = 63 GeV to check the functioning of the apparatus and the analysis.

The experimental apparatus (fig. 1) consisted of two sets of hodoscopes located symmetrically in each arm, downstream from the intersection region. Each of two small-angle hodoscopes (TB) comprised three components (fig. 1b). Two planes of scintillation counters (TBφ) provided a trigger and off-line identification of the doubly charged α particles through pulse-height analysis. The horizontal position of a particle impinging on the hodoscope was determined by arrays of "finger" counters (TBy), 25 mm wide, and the vertical position by two planes of drift tubes (TBz). Each drift tube [1] was a cylinder 10 mm in diameter and 300 mm in length, with 250 μm aluminium walls and a 40 μm diameter sense wire along the axis of the cylinder. The two planes, each of 12 tubes, were staggered vertically to resolve up/down ambiguities. The system was located 8.40 m from the intersection point and subtended the angular range $3.5 < \theta < 16$ mrad. The lower limit corresponded to $|t|$ values of 0.05 and 0.12 GeV^2 for α and p beams.

The hodoscopes H_3 and H_4 were roughly circular, covering the angular region $25 < \theta < 130$ mrad. The fourfold coincidence $(H_3 \cdot H_4)_L \cdot (H_3 \cdot H_4)_R$ served as a luminosity monitor, which had monitor cross-sections of 164, 68, and 24 (±5%) mb for αα, αp, and pp, when calibrated using the standard Van der Meer method [2]. The same hodoscopes were also used in the trigger logic to veto events with secondaries at large angles. The rejection factors of this veto were 10:1 for αα and 4:1 for αp, thus enhancing the fraction of elastic events in the collected data. (We have verified in special runs that < 1% of elastic events were lost due to this requirement).

Alpha-particles were clearly resolved from singly charged particles by imposing cuts in the pulse-height distributions of both planes of a TBϕ hodoscope. (Figure 2 shows one such distribution: in addition to the singly charged and doubly charged single-particle peaks, one also sees a small peak corresponding to two singly charged particles.)

For the results presented in this letter, the requirement was made that the α or p be detected in the central element of the TBy hodoscope, at least on one side.

A candidate track in the drift tubes was defined by the following criteria:

i) counts were required in an overlapping pair of tubes, one in each plane, and

ii) the sum of the drift times in adjacent planes had to correspond to the displacement of the planes, i.e. the radius (5 mm) of a tube.

Finally, elastic events were selected by requiring the collinearity of the left-arm track, the interaction diamond, and the right-arm track. The resolution in collinearity was $\Delta\theta = 0.5$ mrad, mainly determined by the finite dimensions of the source.

This resolution was adequate to discriminate against a potentially troublesome source of background: events in which the α was excited in the collision and decayed into ^{3}He + n. Using a simple Monte Carlo calculation, we found that such a process would result in a flat collinearity distribution with a width of 5 mrad, and estimated the ^{3}He content of our data to be < 5%. Furthermore, one expects the processes $\alpha^* \rightarrow {}^3$He + n and $\alpha^* \rightarrow {}^3$H + p to proceed at more or less the same rate. Since the latter process contributed to the small central peak in the TBϕ pulse-height distribution corresponding to two singly charged particles, we were able to confirm our estimate of the ^{3}He background from the size of this peak.

The analysis outlined above was complicated by δ-ray production, which was manifested in one of two ways. Delta-rays could produce spurious hits in tubes other than the one containing the trigger track (15% of α events). Alternatively, a δ-ray could be detected in the same cell as the triggering particle, resulting in a drift-time sum inconsistent with criterion (ii) above (30% of α events).

Such events were excluded from the final sample, and a correction factor was applied to the resulting $d\sigma/dt$. This correction factor was calculated by assuming that all events which passed the pulse-height cut and which had at least one pair of tracks collinear with the source were elastic events. The value of the correction factor was found not to depend on t.

In figs. 3a-3c we present $d\sigma/dt$ for $\alpha\alpha$, αp, and pp elastic scattering. (In these figures the errors are statistical only.) The major contributions to overall scale errors are:

i) uncertainty in the correction factor applied to the data (30%, 25%, and 10% for $\alpha\alpha$, αp, and pp),

ii) uncertainty in the solid angle (10%), due mainly to the finite size of the source, and

iii) uncertainty in the integrated luminosity (5%).

The resolution in t was ±0.02, ±0.02, and ±0.01 GeV^2 for $\alpha\alpha$, αp, and pp, and only slightly dependent on t, being somewhat better at lower t. This resolution was determined largely by the width of the TBy counters and the horizontal extent of the interaction diamond.

For the pp data, $d\sigma/dt$ (fig. 3c) exhibits a slope parameter $b = 13.2 \pm 0.6$ GeV^{-2} in the range $0.02 < |t| < 0.07$ GeV^2, reproducing well the best ISR result [3] of $b = 13.3 \pm 0.3$ GeV^2 in the same t range. Using the optical theorem and the measured real part of the forward scattering amplitude, we obtained a total cross-section $\sigma_{tot}(pp) = 42.2 \pm 3.5$ mb, which corresponds well to the CERN-Pisa-Roma-Stony Brook result [4] of $\sigma_{tot}(pp) = 43.04 \pm 0.30$ mb. (The errors quoted on σ_{tot} for all three interactions *include* scale errors.)

The differential $\alpha\alpha$ cross-section at $\sqrt{s} = 126$ GeV (Fig. 3a) has a first minimum at $|t| = 0.10 \pm 0.01$ GeV^2 and a second at $|t| = 0.38 \pm 0.02$ GeV^2. Approximating the behaviour at small $|t| = 0.05 - 0.07$ GeV^2 by an exponential (e^{bt}), one obtains a steep slope of $b = 100 \pm 10$ GeV^{-2}. Being determined close to a minimum, this slope is not expected to persist to $|t| = 0$ GeV^2; therefore the estimate of $\sigma_{tot}(\alpha\alpha)$ obtained by extrapolating this slope is unreliable. The resulting value of ≃ 500 mb can only be regarded as an upper limit.

To obtain a more reliable estimate of the αα total cross-section, we parametrized the scattering amplitude as the sum of two interfering exponentials, in the spirit of rescattering models. The resulting five-parameter fit yielded $\sigma_{tot}(\alpha\alpha) = 250 \pm 50$ mb and $\sigma_{el}(\alpha\alpha) = 45 \pm 15$ mb. Another independent estimate of this cross-section was made based on the measured luminosity-monitor cross-sections. Assuming that the monitor detected the same fraction of the total cross-section for αα interactions as it did for αp (0.52 ± 0.09) and pp (0.57 ± 0.06), we derived $\sigma_{tot}(\alpha\alpha) = 295 \pm 40$ mb from the αα monitor cross-section (168 ± 8 mb).

The αp cross-section at $\sqrt{s} = 89$ GeV (fig. 3b) has a slope $b = 41 \pm 2$ GeV^{-2} for $0.05 < |t| < 0.18$ GeV^2 and a minimum at $|t| = 0.20 \pm 0.02$ GeV^2. The extrapolation of this slope gives $\sigma_{tot}(\alpha p) = 130 \pm 20$ mb via the optical theorem (assuming a negligible real part of the forward amplitude) and $\sigma_{el}(\alpha p) = 20 \pm 4$ mb.

The numerical values of the αα and αp differential cross-sections are listed in Table 1. Table 2 contains a summary of the final results obtained.

Alpha-alpha elastic scattering has been studied at lower energy [5] and at the ISR at higher momentum transfers [6]. The lower-energy data at $\sqrt{s} = 8.8$ GeV exhibit a steep slope at low t, terminating in a minimum at $|t| \simeq 0.1$ GeV^2 with a second minimum at $|t| \simeq 0.4$ GeV^2. The similarity between these data and ours indicates that the s dependence of αα elastic scattering is quite weak.

An αp experiment at FNAL [7], covering the energy range $19 < \sqrt{s} < 57$ GeV and a t range compatible with ours, again found a weak (logarithmic) s dependence of the total cross-section and the forward slope parameter. The extrapolation of their fits to $\sqrt{s} = 89$ GeV is in excellent agreement with our measured values.

In conclusion, we have measured the elastic scattering of αα and αp at the highest energies so far available. In αp, the slope and the total cross-section were found to agree with the logarithmic extrapolation of FNAL data. Such a detailed interpretation in the αα case requires more lower-energy data; however, a comparison with very low-energy data indicates that the s dependence of the interaction is weak.

The results reported here were obtained during the initial phase of the experiment before the installation of the entire detector [8]. If, as has been proposed, there is a repetition of α running at the ISR at the end of the year, we shall be able to elicit additional and more precise information concerning the interactions of α's.

Acknowledgements

We are grateful to E. Gabathuler and A. Wetherell for their encouragement and support during the planning and the course of this experiment. We also thank E. Fagiolo and L. Giacomelli of Pisa and especially A. Donnini of the ISR Experimental Support Group for their skilful and enthusiastic technical support.

REFERENCES

[1] U. Becker et al., Nucl. Instrum. Methods 180 (1981) 61.

[2] S. Van der Meer, CERN Internal Report ISR-PO/68-31 (1968).

[3] U. Amaldi et al., Phys. Lett. 66B (1977) 390.

[4] U. Amaldi et al., Phys. Lett. 62B (1976) 460; and Nucl. Phys. B145 (1978) 367.

[5] J. Berger et al., Nucl. Phys. A338 (1980) 421.

[6] M.A. Faessler et al., Preliminary results presented at the 9th Int. Conf. on High-Energy Physics and Nuclear Structure, Versailles, 1981 [published in Nucl. Phys. A374 (1982) 461c].

[7] A. Bujak et al., Phys. Rev. D23 (1981) 1895. The authors found $b_{|t|\simeq 0.1} = 28.6 + 1.32 \ln (s/1\ \mathrm{GeV}^2)$ (GeV^{-2}) and $\sigma_{tot}(\alpha p) = 108.7 + 2.0 \ln (s/1\ \mathrm{GeV}^2)$ (mb). They also found the real part of the forward scattering amplitude to be small.

[8] G. Carboni et al., Phys. Lett. 108B (1982) 145.

Table 1

Differential cross-sections

$\alpha\alpha \to \alpha\alpha$ at $\sqrt{s}$ = 126 GeV			
$\|t\|$ (GeV^2)	$d\sigma/dt$ (mb/GeV^2)	$\|t\|$ (GeV^2)	$d\sigma/dt$ (mb/GeV^2)
0.056	42.4 ± 0.4	0.214	2.16 ± 0.10
0.059	28.0 ± 0.4	0.223	1.72 ± 0.10
0.060	23.0 ± 0.3	0.232	1.40 ± 0.10
0.063	19.4 ± 0.3	0.239	1.20 ± 0.08
0.069	14.0 ± 0.3	0.246	1.10 ± 0.06
0.073	10.8 ± 0.3	0.254	0.92 ± 0.04
0.081	8.5 ± 0.2	0.264	0.80 ± 0.04
0.085	7.8 ± 0.2	0.271	0.64 ± 0.04
0.090	7.4 ± 0.2	0.280	0.55 ± 0.03
0.095	6.8 ± 0.2	0.286	0.42 ± 0.03
0.103	6.9 ± 0.2	0.298	0.34 ± 0.03
0.107	6.1 ± 0.2	0.310	0.28 ± 0.03
0.111	8.1 ± 0.2	0.322	0.18 ± 0.02
0.116	8.5 ± 0.2	0.340	0.144 ± 0.020
0.122	8.4 ± 0.2	0.360	0.104 ± 0.016
0.127	9.2 ± 0.2	0.382	0.050 ± 0.010
0.132	8.7 ± 0.2	0.410	0.058 ± 0.010
0.139	8.0 ± 0.2	0.440	0.068 ± 0.012
0.145	7.1 ± 0.2	0.480	0.040 ± 0.008
0.156	6.0 ± 0.2	0.514	0.028 ± 0.006
0.166	5.5 ± 0.2	0.548	0.028 ± 0.008
0.175	4.5 ± 0.2	0.583	0.024 ± 0.007
0.182	4.0 ± 0.2	0.624	0.018 ± 0.006
0.190	3.6 ± 0.2	0.676	0.018 ± 0.006
0.196	3.20 ± 0.14	0.720	0.009 ± 0.003
0.206	2.60 ± 0.14		
$\alpha p \to \alpha p$ at $\sqrt{s}$ = 89 GeV			
$\|t\|$ (GeV^2)	$d\sigma/dt$ (mb/GeV^2)	$\|t\|$ (GeV^2)	$d\sigma/dt$ (mb/GeV^2)
0.052	97.5 ± 2.0	0.127	3.3 ± 0.4
0.056	86.2 ± 2.0	0.133	3.9 ± 0.4
0.060	81.1 ± 1.8	0.144	1.7 ± 0.3
0.063	69.8 ± 1.7	0.149	2.0 ± 0.3
0.067	60.5 ± 1.6	0.155	1.3 ± 0.2
0.071	46.2 ± 1.4	0.161	1.2 ± 0.2
0.075	41.2 ± 1.3	0.167	1.1 ± 0.2
0.079	31.2 ± 1.1	0.174	0.96 ± 0.20
0.084	24.8 ± 1.0	0.180	0.46 ± 0.12
0.088	20.4 ± 0.9	0.186	0.38 ± 0.12
0.099	13.8 ± 0.4	0.193	0.25 ± 0.16
0.112	10.7 ± 0.7	0.210	0.48 ± 0.12
0.117	8.2 ± 0.6	0.220	0.80 ± 0.18
0.122	6.1 ± 0.5	0.228	1.08 ± 0.20

Table 2

Summary of the results

	$\alpha\alpha \rightarrow \alpha\alpha$	$\alpha p \rightarrow \alpha p$	$pp \rightarrow pp$
$\sqrt{s}$ (GeV)	126	89	63
b (GeV^{-2}) in $\|t\|$ range (GeV^2)	100 ± 10 0.05 - 0.07	41 ± 2 0.05 - 0.18	13.3 ± 0.6 0.02 - 0.07
$\|t\|_{1st\,min}$ (GeV^2)	0.10 ± 0.01	0.20 ± 0.01	---
$\|t\|_{2nd\,min}$ (GeV^2)	0.38 ± 0.02	---	---
σ_{tot} a) (mb)	250 ± 50 b) 295 ± 40 c)	130 ± 20	42.2 ± 3.5
σ_{el} a) (mb)	45 ± 15 b)	20 ± 4	---

a) Errors include scale errors.

b) Based on fit.

c) Based on monitor cross-section.

Figure captions

Fig. 1 : The experimental apparatus:

a) plan view,

b) exploded view of the TB hodoscopes.

Fig. 2 : Typical pulse-height distribution for one of the TBϕ counters.

Fig. 3 : The measured elastic cross-sections $d\sigma/dt$:

a) $\alpha\alpha \rightarrow \alpha\alpha$ at $\sqrt{s}$ = 126 GeV (over-all scale error: 32%).

b) $\alpha p \rightarrow \alpha p$ at $\sqrt{s}$ = 89 GeV (over-all scale error: 27%).

c) $pp \rightarrow pp$ at $\sqrt{s}$ = 63 GeV (over-all scale error: 15%).

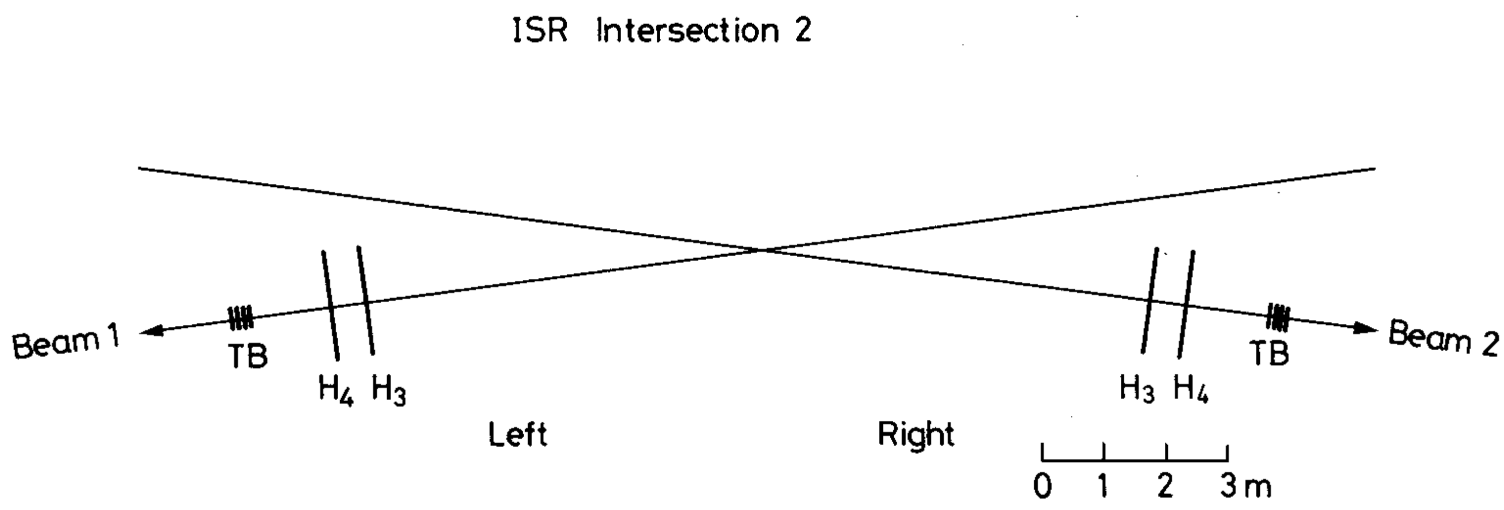
ISR Intersection 2
Beam 1
TB
H4 H3
Left
Right
H3 H4
TB
Beam 2
0 1 2 3 m

Fig. 1a

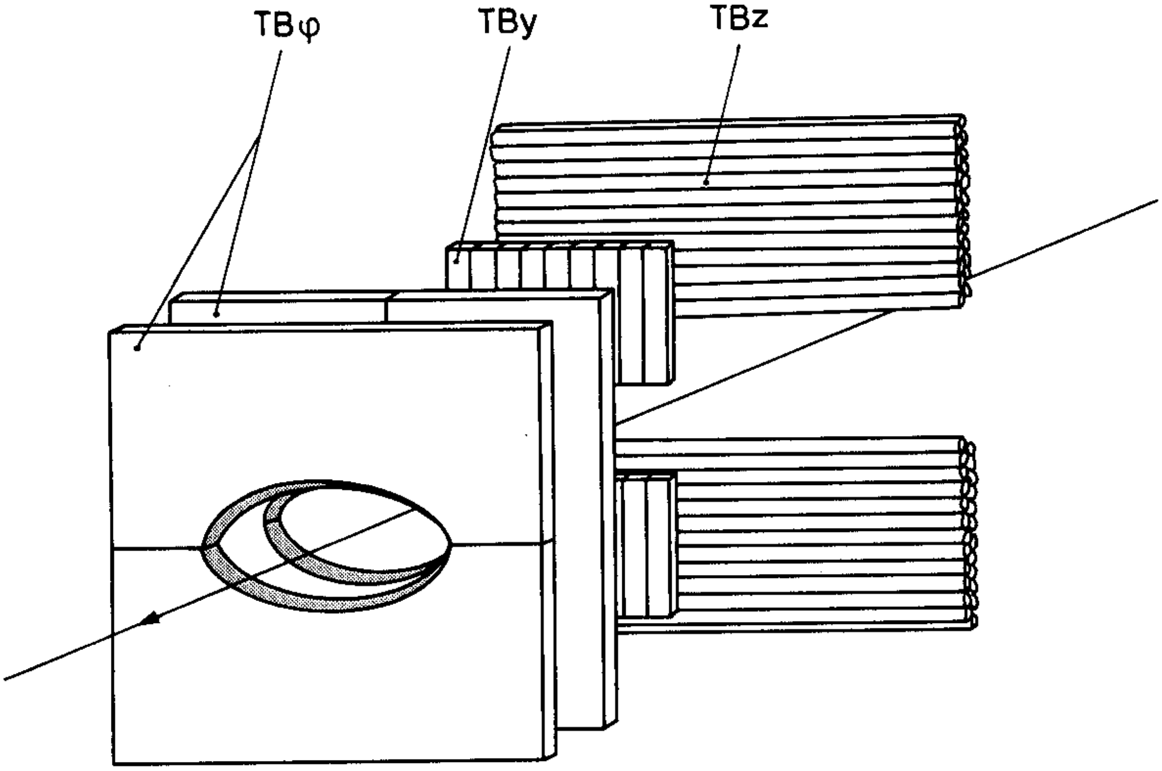

Fig. 1b

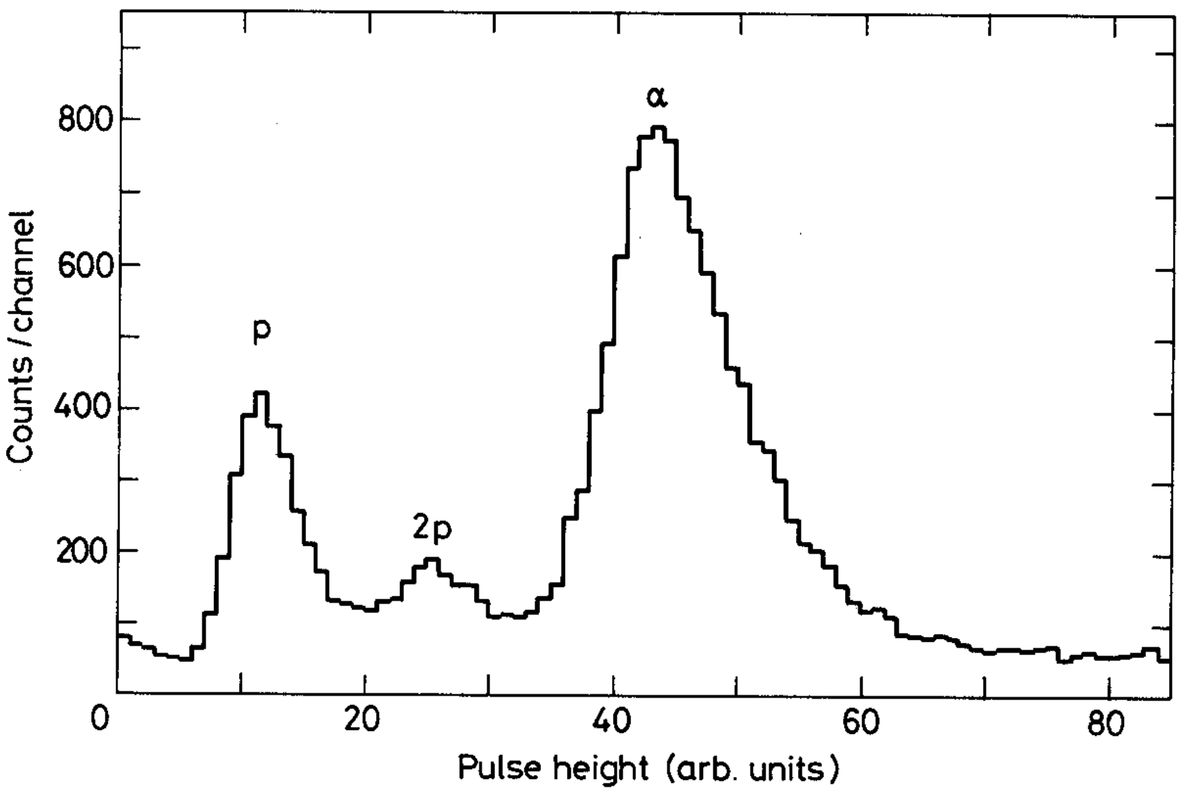

α
p
2p
Counts / channel
800
600
400
200
0
20
40
60
80
Pulse height (arb. units)

Fig. 2

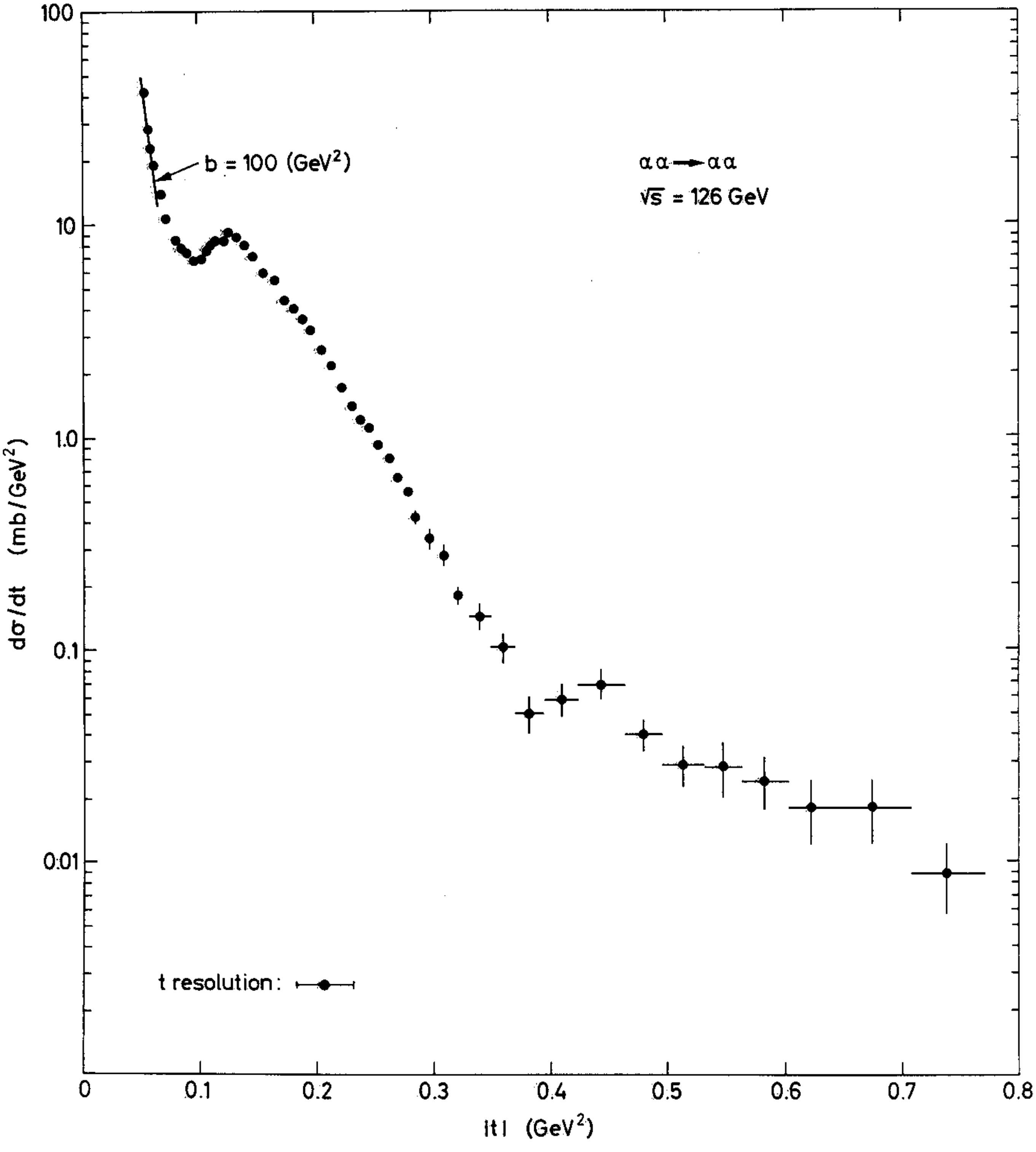

100
10
1.0
0.1
0.01
dσ/dt (mb/GeV^2)
b = 100 (GeV^2)
αα → αα
√s = 126 GeV
t resolution:
0
0.1
0.2
0.3
0.4
0.5
0.6
0.7
0.8
|t| (GeV^2)

Fig. 3a

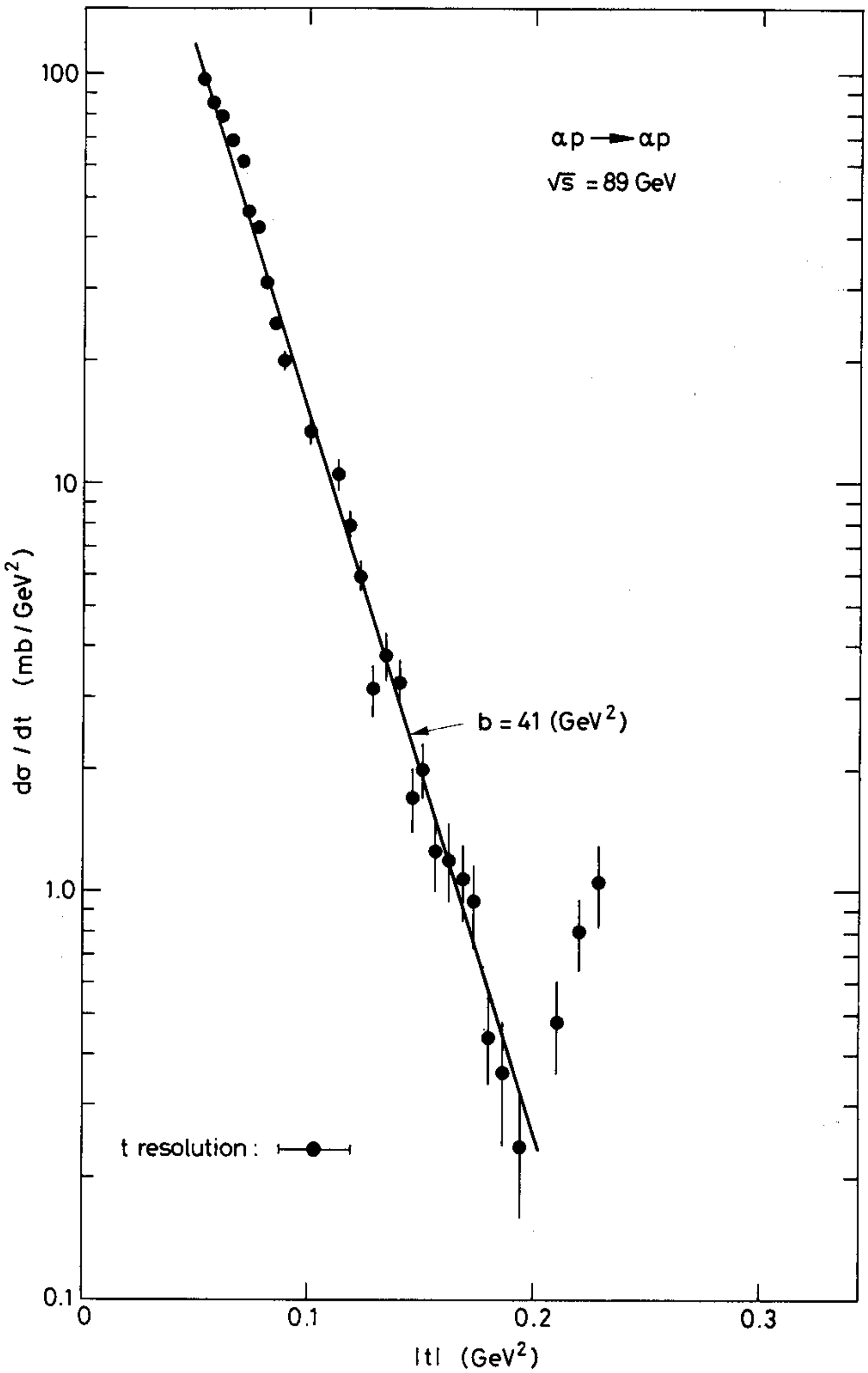

100
10
1.0
0.1
0
0.1
0.2
0.3
dσ / dt (mb / GeV²)
|t| (GeV²)
αp → αp
√s = 89 GeV
b = 41 (GeV²)
t resolution :

Fig. 3b

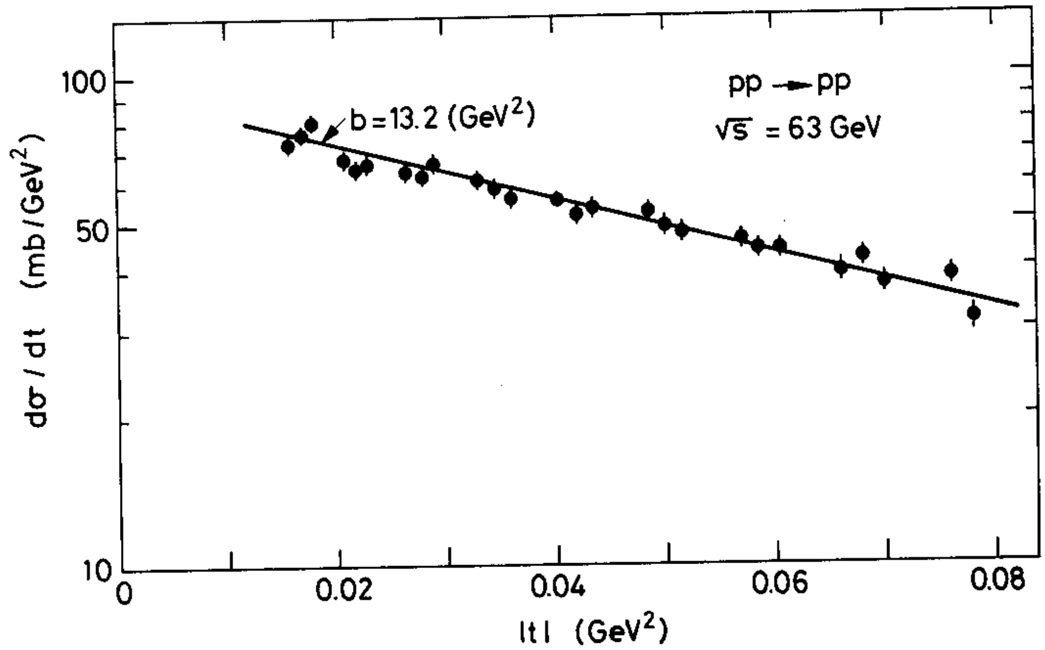

100
50
10
dσ / dt (mb/GeV²)
b = 13.2 (GeV²)
pp → pp
√s = 63 GeV
0
0.02
0.04
0.06
0.08
|t| (GeV²)

Fig. 3c